HHS Public Access

Author manuscript

Kidney Int. Author manuscript; available in PMC 2017 May 01.

Published in final edited form as:

Kidney Int. 2016 May ; 89(5): 1027–1036. doi:10.1016/j.kint.2015.12.046.

Osteopontin protects against high phosphate-induced nephrocalcinosis and vascular calcification

Neil J. Paloian[1], **Elizabeth M. Leaf**[2], and **Cecilia M. Giachelli**[2]

[1]Pediatrics, University of Wisconsin School of Medicine and Public Health

[2]Bioengineering, University of Washington

Abstract

Pathologic calcification is a significant cause of increased morbidity and mortality in patients with chronic kidney disease (CKD). The precise mechanisms of ectopic calcification are not fully elucidated, but it is known to be caused by an imbalance of pro-calcific and anti-calcific factors. In the CKD population, an elevated phosphate burden is both highly prevalent and a known risk factor for ectopic calcification. Here we tested whether osteopontin, an inhibitor of calcification, protects against high phosphate load-induced nephrocalcinosis and vascular calcification. Osteopontin knockout mice were placed on a high phosphate diet for eleven weeks. Osteopontin deficiency together with phosphate overload caused uremia, nephrocalcinosis characterized by substantial renal tubular and interstitial calcium deposition, and marked vascular calcification when compared to controls. While the osteopontin-deficient mice did not exhibit hypercalcemia or hyperphosphatemia, they did show abnormalities in the mineral metabolism hormone fibroblast growth factor 23. Thus, endogenous osteopontin plays a critical role in the prevention of phosphate induced nephrocalcinosis and vascular calcification in response to high phosphate load. A better understanding of osteopontin's role in phosphate induced calcification will hopefully lead to better biomarkers and therapies for this disease, especially in patients with CKD and other at risk populations.

Keywords

vascular calcification; phosphate; calcium; FGF23; parathyroid hormone; uremia

Introduction

Pathologic calcification of soft tissues has deleterious effects depending on the organ system involved. Nephrocalcinosis is the deposition of calcium within the renal parenchyma and

Address for Correspondence: Cecilia Giachelli, Department of Bioengineering, University of Washington, 3720 15th Ave NE, Foege N330L, Box 355061, Seattle, WA 98195, phone: 206-543-0205, fax: 206-616-9763, ceci@uw.edu.

Disclosure

All authors have no competing interests.

tubules. This accumulation of calcium in the kidney is due to increased urinary excretion of calcium, phosphorus, and/or oxalate in combination with a loss of protective urinary inhibitors of mineralization. There are many underlying diseases that cause nephrocalcinosis and depending on the etiology, nephrocalcinosis can cause progressive renal dysfunction and end stage renal disease (ESRD)[1]. Similar to nephrocalcinosis, vascular calcification (VC) is caused by an imbalance in pro-calcific and anti-calcific factors. In the vasculature, calcification is associated with increased cardiovascular morbidity and mortality[2, 3]. While VC is seen as a component of aging, the increased cardiac risk is especially prevalent in certain disease states such as diabetes mellitus (DM) and chronic kidney disease (CKD)[4–6]. VC can involve either the intimal or medial layer of the arterial wall. Intimal calcification is typically secondary to atherosclerosis while medial calcification is much more characteristic of patients with DM and CKD[7–10]. Once thought to be a benign finding, arterial medial calcification is associated with increased vessel wall stiffness, decreased vascular compliance, increased pulse wave velocity and systolic hypertension[11, 12]. Together these symptoms lead to decreased coronary perfusion, left ventricular hypertrophy and eventually to congestive heart failure or myocardial infarction[13]. The mainstay of VC therapy involves attempting to maintain mineral homeostasis with the use of oral phosphate binders, activated vitamin D or vitamin D analogs, and calcimimetics, but at present there is no effective treatment for this disease.

An elevated phosphate load is a known risk factor for the development of both renal and vascular calcification. Administration of high doses of phosphate to rodents causes nephrocalcinosis and significant renal damage[14, 15]. A higher phosphate diet leads to urinary calcium phosphate supersaturation and an increase in calcium phosphate kidney stones in settings of genetic hypercalciuria[16]. In humans, elevated phosphate loading from colonoscopy preps or tumor lysis syndrome causes phosphate nephropathy and acute kidney injury, which is now known to be a major risk factor for the development of CKD[17–19]. In uremic animal models phosphate loading is known to cause VC and in patients with pre-existing CKD, hyperphosphatemia is a significant risk factor for VC and for cardiovascular mortality[20–22]. Even in patients without CKD, elevated serum phosphate levels are associated with increased cardiovascular risk[23]. This is particularly concerning as the phosphorus content of the US food supply continues to increase and correlates with the rising use of phosphate additives, which are mostly inorganic phosphate salts with rapid intestinal absorption and high bioavailability[24].

The underlying mechanisms that lead to pathologic calcification are complex and thought to involve active, regulated processes that are common to bone formation. Loss of anti-calcific factors is considered a critical element contributing to both bone mineralization and pathologic calcification[25]. One important anti-calcific protein is osteopontin (OPN). OPN, a multifunctional phosphoprotein and member of the ‘SIBLING’ (small integrin-binding ligand N-linked glycoproteins) family, was initially discovered as a major non-collagenous component of cortical bone[26]. OPN is produced by multiple cell types in bone and plays an integral role in bone remodeling largely due to its function in osteoclast adhesion and bone resorption[27]. Osteopontin is rich in aspartic acid, glutamic acid, a polyaspartic acid motif, and can be highly phosphorylated at serine and threonines, all of which allows it to bind to both ionic calcium and to hydroxyapatite, making it a potent inhibitor of calcification[28–30].

As OPN is a multifunctional protein, it has been studied in a wide range of disease models including cancer, osteoporosis, liver disease, and infectious diseases, but despite the large number of studies utilizing OPN deficient mice, spontaneous vascular calcification has never been described in these animals.

Another important molecule involved in mineralization is Fibroblast Growth Factor-23 (FGF-23), which is primarily produced by osteocytes and functions to maintain phosphorus homeostasis in the body[31]. Increased phosphorus and 1,25$(OH)_2$D stimulate FGF-23 release from osteocytes under the control of PHEX and DMP1 proteins[32]. Intact FGF-23 binds with its co-receptor α-klotho, which is secreted by renal tubular cells, and this complex activates FGF receptors (FGFR) in the renal proximal tubule and reduces expression of the type II sodium/phosphate co-transporters (NaPi2)[33]. In this fashion, FGF-23 prevents hyperphosphatemia by decreasing urinary phosphate reabsorption. This effect is recognized prominently in CKD, where FGF-23 levels increase to counter decreased glomerular filtration of phosphorus as glomerular filtration rate (GFR) declines[34]. FGF-23 also inhibits CYP27B1 (25-hydroxyvitamin D 1α hydroxylase) decreasing the production of 1,25 $(OH)_2$D and stimulates CYP24A1 (1,25-dihydroxyvitamin D 24-hydroxylase) increasing the conversion of 1,25 $(OH)_2$D into inactive metabolites[35].

The aim of the present study was to determine whether endogenous OPN has a protective role in renal and vascular calcification in the setting of a high phosphate load. To test this, OPN knockout mice were exposed to a high phosphate burden by placement on a high phosphate diet. We discovered that these mice developed both extensive renal and vascular calcification as well as aberrations in serum FGF-23 levels compared to wildtype mice. The data suggest that OPN has a major renal and vascular protective effect against ectopic calcification induced by high phosphate loading.

Results

Renal insufficiency and altered mineral metabolism in high phosphate-fed OPN KO mice

Serum chemistries were determined at termination and are shown in Table 1. BUN (blood urea nitrogen) levels of the WT+NP and KO+NP groups were not significantly different. HP feeding alone did not lead to significant increases in BUN in WT mice (compare WT+NP group to the WT+HP group). In contrast, the KO+HP group had elevated BUN (36 mg/dL), which was significantly higher when compared to all other groups, demonstrating renal insufficiency in these mice. The only difference in serum calcium levels were between the KO+NP and KO+HP groups, with the KO+HP group demonstrating lower calcium levels than the KO+NP group. Serum phosphorus levels were lower in both HP fed mice compared to their genotypic equivalent NP fed mice. There were no differences in phosphorus levels when comparing mice between genotypes given the identical dietary phosphate load. Parathyroid hormone (PTH) levels in the KO+HP group were significantly higher than the WT+NP group but there were no other differences between groups. FGF-23 levels were significantly elevated in the KO+HP group compared to all other groups. It is noteworthy that FGF-23 levels were significantly higher in the KO+HP group compared to the WT+HP group, and, although not reaching statistical significance, FGF-23 levels trended higher in the KO+NP group compared to the WT+NP group.

OPN-null mice on high phosphate diet develop renal and vascular calcification

Renal histology and IF were performed to characterize renal morphology in all groups. H&E staining of the kidneys was normal in both WT+NP and KO+NP groups. The WT+HP group demonstrated some abnormalities including mild interstitial inflammation and some subcapsular inflammation. This was more pronounced in the KO+HP group with marked presence of inflammatory cells surrounding tubular mineral deposits and some of the more cystic, dilated glomeruli (Figure 1, panels A–D). Tubular mineral deposits were also frequently seen on the KO+HP group with H&E staining (Figure 1, arrowhead in panel D). PAS staining demonstrated normal morphology in both NP groups. The WT+HP group showed occasional tubular dilatation but this again was more prominent in the KO+HP group which contained many dilated and degenerative tubules along with some cystic appearing glomeruli (Figure 1, panels EH). Occasional tubular mineral deposits were also noted in the WT+HP group (Figure 1, arrowhead in panel G). To confirm the presence of inflammatory cells, CD45 IF was performed on adjacent kidney sections. Both NP groups showed an occasional inflammatory cell throughout the kidney sections. CD45 IF confirmed the mild interstitial and subcapsular inflammation in the WT+HP group. As expected, the KO+HP group displayed massive areas of CD45+ inflammatory infiltrate, which surrounded tubules and calcified deposits (Figure 1, panels I–L). Von Kossa staining was performed to detect the presence of phosphate deposition in the kidneys. VK staining did not detect any mineralization in either the WT+NP and KO+NP groups. The WT+HP group did exhibit occasional areas of phosphate deposition and these were confined to the renal tubules. In comparison, the KO+HP group showed a substantial amount of mineral deposition in the tubules. There was also positive VK staining seen intermittently in the renal parenchyma (Figure 2.i). The VK scores were also higher in the KO+HP group signifying increased calcium deposits (Figure 2.ii). OPN IHC demonstrated abundant OPN expression in the renal tubular cells of both WT groups and the absence of OPN in the KO groups as expected (Figure 3).

To determine the role of OPN in VC, calcium content of the aortic arch and lower abdominal aorta was determined. The total combined calcium content of the aortic arch plus the lower abdominal aorta in the KO+HP group was over 6 fold higher than the WT+HP group with average tissue calcium levels of 18.9 ± 5.0 μg calcium/mg dry tissue weight vs 2.9 ± 0.5 μg calcium/mg dry tissue weight respectively. Calcium content of the aortic arch plus the lower abdominal aorta in both of the NP groups was low with 2.3 ± 0.9 μg calcium/mg dry tissue weight in the WT+NP group and 1.3 ± 0.6 μg calcium/mg dry tissue in the KO+NP group (Figure 4.i).

Arterial calcification was also evaluated histologically by examining cross sections of abdominal aorta. H&E staining demonstrated normal vascular architecture of the WT+NP, KO+NP, and WT+HP groups. Examination of KO+HP group by H&E showed straightening of elastic fibers with no atherosclerotic lesions at areas of calcification (data not shown). Advanced vascular mineral deposits in the KO+HP group were positive for Alizarin Red as shown in Figure 4.ii. These calcifications were confined exclusively to the medial layer of the vessel. AR staining did not detect aortic mineralization in any of the remaining three groups including the WT+HP group. SM22α IHC was positive in aortic sections along the

entirety of the medial layer in the WT+NP, KO+NP, and WT+HP groups (Figure 5). In the KO+HP group SM22α was absent in large segments of the medial layer correlating with areas of mineralization. As expected, OPN IHC did not detect OPN in the vasculature of either of the WT groups nor the KO+NP group, due to the lack of mineralization. No OPN was detected in the KO+HP group as expected despite the presence of mineral in the vessel wall (Figure 6).

Increased production of FGF-23 by bone in OPN KO mice

FGF-23 expression in osteocytes was assessed by performing immunofluorescence (IF) on femurs from study mice from all four groups. FGF-23 expression examined by IF was noted to be markedly increased in both HP groups with the KO+HP group showing the highest number of FGF-23 positive osteocytes (Figure 7i). As seen on H&E femur sections, both HP groups displayed wider diaphyseal cortical bone and cortical porosity (Figure 7ii, panels C & D) indicative of remodeling. Interestingly, the KO+HP group showed multiple, large trabecular protrusions that contained many positive FGF-23 cells (Figure 7ii, panels D & H). Representative FGF-23 IF micrographs are shown in Figure 7ii, panels E – H. There were no abnormalities in H&E femur sections from the NP groups (Figure 7ii, panels A & B) and no appreciable difference in FGF-23 expression between the WT+NP and KO+NP groups (panels E & F).

Discussion

Our study demonstrates that high phosphate feeding in the setting of OPN deficiency leads to nephrocalcinosis, uremia, and vascular calcification in mice. While other experimental models have clearly demonstrated OPN's anti-calcific property, our findings are unique in that they establish OPN as a simultaneous protector of both vascular and renal calcification. This is particularly noteworthy as clinical studies show a strong correlation between kidney stone formation and VC, and pathogenic links between nephrocalcinosis and VC have been hypothesized[1, 36]. Also, previous *in vivo* calcification models utilizing OPN KO animals have induced calcification in various ways such as graft implantation or oxalate administration (given orally or via injection)[37–39]. While both of these scenarios are of clinical importance, our study is the first to show significant calcification with oral phosphate administration. With the growing use of phosphate-based food additives and the further comprehension of phosphate as a vascular toxin, it is critical to fully understand the interaction of phosphate and OPN in ectopic calcification.

Both wildtype and OPN knockout mice placed on the high phosphate diet developed renal tubular phosphate deposition, but this was much more severe in the OPN knockout mice and correlated with worsening uremia. Wild type mice on a high phosphate diet had no signs of arterial calcification; the combination of OPN deficiency and a high phosphate load led to significant VC, which was located entirely in the medial layer of the artery consistent with pathologic states such as CKD. Calcium and phosphorus levels fluctuated somewhat across the study groups but the OPN+HP group affected with calcification and uremia did not demonstrate hypercalcemia or hyperphosphatemia. As expected, FGF-23 and PTH levels

were highest in the HP fed groups with FGF-23 levels significantly elevated in the KO+HP mice.

Our findings are consistent with previous studies showing that OPN is a potent inhibitor of *in vitro* and *in vivo* calcification. In the kidney, OPN is normally expressed in the renal tubule with highest concentrations in the distal tubule and is an important inhibitor of renal calcium-containing crystal formation[40, 41]. This was demonstrated by *Mo et al* who discovered that OPN-null mice developed spontaneous renal calcification at a rate of 10% which increased to 65% when challenged with ethylene glycol[37]. While the previous study examined renal calcium oxalate deposition, our studies are consistent with their findings, and indicate that the absence of OPN aggravates pathologic mineralization of the kidney also under the condition of elevated phosphate loading. Interestingly, we observed no evidence of spontaneous ectopic calcium deposition in the OPN-null mice on a standard phosphate diet. Our studies are also in agreement with other published data examining the protective role of OPN on vascular smooth muscle calcification. The addition of OPN to vascular smooth muscle cells (VSMCs) grown in a pro-calcific media dose dependently inhibits calcification and when VSMCs obtained from OPN knockout mice are cultured, the cell cultures demonstrate enhanced susceptibility to calcification[42, 43]. In an *in vivo* model, Kaartinen *et al* revealed that OPN is up regulated in the calcified arteries of MGP-null mice[44]. In addition, 3 different OPN double knockout mouse models (with MGP, ApoE, and LDLR) have been created and developed more vascular calcification than the original knockout mouse with OPN intact[45–47]. Together, these studies support the idea that endogenous OPN protects against renal and vascular calcification.

Our findings of a protective role of OPN against HP-induced renal calcification is particularly important as there has been growing evidence linking abnormal renal calcification and loss of renal function. In analyses of CKD patients, especially those at very high risk for developing ectopic calcification, there was a clear association between altered mineral metabolism and progressive loss of renal function[48, 49]. Phosphate nephropathy and nephrocalcinosis are also likely under-recognized causes of ongoing loss of GFR[50, 51]. A recent study by *Evenepoel et al* demonstrated that microscopic nephrocalcinosis was quite common in patients with CKD and prevalence increased with worsening glomerular filtration rate and correlated with elevated serum phosphate and parathyroid hormone levels[52]. It is likely that OPN is involved in this process as *Lorenzen et al.* discovered that OPN levels increased with worsening GFR[53]. These increased levels also correlated closely with serum phosphate and intact parathyroid hormone. Comparable findings by *Barreto et al* in CKD patients and *Yamaguchi et al* in diabetic patients with renal failure demonstrated increased serum OPN levels that associated with loss of renal function[54, 55]. It is likely that OPN levels increase to offset further pathologic renal calcification as OPN is upregulated at sites of pathologic calcification. This was first described by *Giachelli et al* in 1993 when OPN (not normally found in the vasculature) was detected at sites of human atherosclerosis and seen most prominently at regions of intimal calcification[56]. In the rat kidney, *Matsuzaki et al* demonstrated that a high phosphate diet induces expression of OPN in the renal tubules[57]. Since the OPN KO mice in our study were incapable of expressing or upregulating OPN under the stimulus of a high phosphate load, they were highly susceptible to developing ectopic calcification. This mechanism of amelioration of pathologic

mineralization by OPN may underlie the elevated OPN levels observed in CKD patients, although OPN's utility as a biomarker or therapeutic is still unclear.

One surprising finding of this study was the development of glomerular cysts in the OPN KO+HP mouse. Cystic glomeruli are seen in multiple different clinical scenarios, but many involve abnormal development of the glomerulus either from genetic disorders or from fetal urinary obstruction. While this has not been commonly described in cases of adult nephrocalcinosis or nephrolithiasis, this has been observed in multiple animal models of induced tubulointerstital disease, the most recent by Schulte et al in which glomerular detubularization and atubular glomeruli were produced by electrocoagulation[58]. This resulted in significant development of glomerular cysts in affected tubules, similar to results seen by our experimental model. The significant inflammatory cell response seen surrounding dilated renal tubules and crystals in the KO+HP mice supports the idea that severe tubulointerstital disease can lead to the development of post-natal glomerulocystic kidney disease. This tubulointerstital inflammation along with tubular crystal obstruction has led to uremia in our KO+HP group.

While it is clear that OPN is an important inhibitor of both renal and vascular calcification, it may also be playing a role in the regulation of systemic mineral metabolism. FGF-23 is known to increase in response to a phosphate load and would be expected to be elevated in the mice on the HP diet; however serum FGF-23 was markedly increased in the KO mouse when compared to its diet matched control, suggesting that OPN may normally act to inhibit serum FGF-23 accumulation. A link between OPN and FGF23 levels has also been reported by *Yuan et al,* who found that FGF-23 null mice, while having hyperphosphatemia and a skeletal mineralization defect, displayed elevated levels of OPN both in bone and serum[59]. In addition, *Kodek et al* noted that PHEX, which is involved in FGF-23 release, also regulates the OPN ASARM (acidic serine- and asparate-rich motif) peptides responsible for phosphorylation-dependent mineralization inhibition[60]. Based on our finding of a notable increase in the number of osteocytes expressing FGF-23 in the KO+HP mouse osteocytes, we propose that OPN is an inhibitor of FGF-23 production at the level of the osteocyte. Loss of OPN allows the high phosphate stimulated release of FGF-23 to proceed uninhibited and causes decreased phosphate reabsorption in the proximal tubule of the nephron and inappropriately increased urinary phosphate excretion in our model.

Serum calcium levels were lowest in the KO+HP mouse group. Both kidney dysfunction and elevated FGF-23 levels together likely lead to the development of hypocalcemia in this cohort. Declining GFR is associated with skeletal resistance to the calcemic activities of PTH and is one of the causes of hypocalcemia in CKD[61]. Also, FGF-23 is known to down regulate the activity of the 1-alpha- hydroxylase enzyme, decreasing conversion of 25-hydroxy vitamin D to 1,25-dihydroxy Vitamin D[35]. Low levels of 1,25-dihydroxy Vitamin D decrease intestinal absorption of calcium; unfortunately we were unable to obtain1,25-dihydroxy Vitamin D levels due to the large volume of serum necessary.

In summary, a high phosphate load in the absence of OPN causes significant renal and arterial mineral deposition, demonstrating OPN's role in the prevention of phosphate induced nephrocalcinosis and vascular calcification. Whether or not OPN therapy would

mitigate nephrocalcinosis, progression of CKD, or VC in at risk groups still needs to be studied.

Materials and Methods

Animal Studies

OPN knockout mice on the DBA/2J background were bred and genotyped in-house as previously described[62]. Diets included a synthetic, normal phosphate (0.5%) diet (NP) or a high phosphate (1.5%) diet (HP) obtained from Dyets Inc., catalog numbers 181084 and 113322 respectively. Both diets had a calcium content of 0.6%. Wild type and knockout mice were placed on either NP or HP diet for 11 weeks and were terminated at the end of the study period. Mice were assigned to the following experimental groups: WT+NP, WT+HP, KO+NP, and KO+HP (n = 10/group). All mice used were normal, adult females. OPN WT control mice were generated from the same breeding and were often littermates of KO mice. Mice had access to food and water *ad libitum* and were maintained according to IACUC policies of the University of Washington, Seattle.

Serum Chemistries

Mice were fasted for 3 hours and terminal blood was collected via cardiac puncture during tissue harvest at the end of the 11-week study period. Whole blood was allowed to clot for one hour and then centrifuged at 3300 rpm for 15 minutes. The resulting serum was then aliquoted. Serum calcium was ascertained using the *o*-cresolphthalein complexone kit for calcium from Teco Diagnostics (catalog # C503-480). Serum BUN was determined using the QuantiChrom™ urea assay kit from BioAssay Systems (catalog # DIUR-500). Serum FGF-23 and PTH analyses were performed using the mouse/rat FGF-23 (C-Term) ELISA kit from Immutopics (catalog # 60-6300) or the mouse PTH 1 – 84 ELISA kit from Immutopics (catalog # 60-2305) respectively. Serum phosphorous was determined using a standard autoanalyzer at Phoenix Central Laboratory (Everett, WA).

Aortic Calcium Quantification

Aortic arches and lower abdominal aortas were collected, lyophilized, and decalcified separately with 0.6N HCl. Calcium content of supernatant was determined for each individual arotic segment using the *o*-cresolphthalein complexone kit from Teco Diagnostics (catalog # C503-480) and calcium content of aortic segments were normalized to the dry weight of the corresponding tissue. The results of the aortic arch and lower abdominal aorta were then added together and expressed as arch plus lower abdominal aorta (μg calcium/mg dry weight).

Histology, Immunofluorescence, and Immunohistochemistry

Upper abdominal aortas were harvested, fixed, and examined for morphology/pathology, calcification, and OPN and SM22α protein content. Kidneys were also harvested and fixed in a similar manner, stained for H&E and PAS, and probed for CD45. Briefly, tissues were fixed in 3:1 methanol:glacial acetic acid for 2 – 4 hours, processed, and sectioned. Paraffin sections of aortas (n = 3/group) were hematoxylin and eosin stained (H&E) for morphology and alizarin red S stained (AR) to locate calcification. OPN immunohistochemistry was

conducted on KO aorta sections that contained mineral ($n = 3$) to also confirm loss of the OPN protein in the presence of calcification. SM22α IHC was performed on all aortic sections. Paraffin sections of kidneys were stained for periodic acid Schiff's (PAS) and H&E for morphology/pathology. CD45 immunofluorescence (IF) was used to identify inflammatory cells in the kidney sections of all groups. von Kossa (VK) staining was utilized to detect calcium phosphate deposits. Black/brown precipitates on VK sections were manually counted on blinded samples and a histochemical score was assigned according to the number of granules in one longitudinal section per mouse. A score of 0 was given for no granules found in the section, a 1 for1–25 granules, a 2 for 26–75 granules, a 3 for 76–150 granules, and a 4 for >150 granules as previously described[63]. Absence of the OPN protein was determined using IHC on all KO kidneys while running WT kidneys as an OPN positive control. Slides of kidney tissue were blinded and kindly observed by Dr. Charles Alpers from the University of Washington for pathological determination.

OPN IHC was carried out on fixed sections embedded in paraffin. Sections were deparaffinized, rehydrated, and blocked with 0.3% hydrogen peroxide in methanol, 4% normal rabbit serum in PBS, and finally with avidin & biotin. Samples were then incubated sequentially with goat anti-mouse OPN primary antibody (R&D Systems, catalog # AF808), rabbit anti-goat biotinylated IgG (Vector Laboratories, catalog #BA-5000), and avidin-biotin-horseradish peroxidase (HRP) complex (Vector Laboratories). The immunohistochemical signal was then visualized with 3,3′-diaminobenzidine (Sigma). Slides were then counterstained with methyl green, dehydrated, and coverslipped. For all samples, negative controls included substitution of the primary antibody with goat isotype non-specific IgG. SM22α IHC was carried out in identical fashion with a goat anti-sm22α primary antibody that reacts with mouse (Abcam, catalog # ab10135). CD45 IF was performed on fixed kidney sections embedded in paraffin. Sections were deparaffinized, rehydrated, and permeabilized with 0.1% Tween 20 in 0.05M Tris and 0.15M NaCl followed by blocking with 4% normal donkey serum diluted in PBS. Kidney sections were then incubated with a monoclonal rat anti-mouse CD45 IgG_{2b}, K (BD Biosciences, catalog # 550539) at 6.25ug/mL followed by incubation with an AffiniPure donkey anti-rat Cy™3-conjugated secondary antibody (Jackson ImmunoResearch, catalog # 712-165-153) at 7.5ug/mL. Nuclei were then counterstained with 300nM 4′, 6-diamidino-2-phenylindole dilactate (DAPI) (Life Technologies, catalog # D3571) and slides were mounted with ProLong Gold antifade media (Life Technologies, catalog # P36930). Negative controls consisted of incubation with isotype specific rat IgG_{2b}, K at 6.25ug/mL instead of the primary antibody. For long bone histology and IF, femurs were harvested and preserved in 70% ethanol at 4°C. Femurs were then fixed in 4% paraformaldehyde at 4°C overnight and decalcified at room temperature for 4 days in Cal-Ex® (Fisher, catalog # CS510-1D). After decalcification, femurs were rinsed with water, stored in 70% ethanol, and then processed & embedded in Paraplast® Plus. Longitudinal sections were cut, stained with H&E, and probed for FGF-23. Femurs sections were incubated with a monoclonal rat anti-mouse FGF-23 IgG_{2A} clone # 283507 (R&D Systems, catalog # MAB26291) at 5ug/mL followed by incubation with an Alexa Fluor® 488-conjugated AffiniPure Donkey Anti-Rat IgG secondary antibody at 7.5ug/mL (Jackson ImmunoResearch, catalog # 712-545-153). Slides were mounted in ProLong Gold antifade media. A monoclonal rat IgG_{2A} isotype control at

5ug/mL (R&D Systems, catalog # MAB006) was used as a negative control for antibody specificity. Femurs stained for FGF-23 were then scored blinded as follows: 0 = no FGF-23 positive cells; + some FGF-23 positive cells in cortical bone; ++ many FGF-23 positive cells in cortical bone; +++ many FGF-23 positive cells in cortical bone and in new trabecular protrusions. Scoring data was then assigned an arbitrary unit and graphed.

Statistical Analysis

All results are displayed as mean ± standard error. Differences between the means of the groups were compared using one-way ANOVA analysis with Tukey post-hoc analysis. A p value of less than 0.05 was considered to be statistically significant. SPSS software v16.0 (SPSS, Chicago, IL) was used for all statistical analysis.

Acknowledgments

Funding for Dr Giachelli's research is supported by NIH grants HL62329, HL081785, and HL114611, and a grant from the DOD PRORP #OR120074. Dr Paloian is supported by NIH 5T32DK7662-22.

References

1. Shavit L, Jaeger P, Unwin RJ. What is nephrocalcinosis? Kidney Int. 2015; 88:35–43. [PubMed: 25807034]
2. Witteman JC, Kok FJ, van Saase JL, et al. Aortic calcification as a predictor of cardiovascular mortality. Lancet. 1986; 2:1120–1122. [PubMed: 2877272]
3. Witteman JC, Kannel WB, Wolf PA, et al. Aortic calcified plaques and cardiovascular disease (the Framingham Study). Am J Cardiol. 1990; 66:1060–1064. [PubMed: 2220632]
4. Adragao T, Pires A, Lucas C, et al. A simple vascular calcification score predicts cardiovascular risk in haemodialysis patients. Nephrol Dial Transplant. 2004; 19:1480–1488. [PubMed: 15034154]
5. Russo D, Corrao S, Battaglia Y, et al. Progression of coronary artery calcification and cardiac events in patients with chronic renal disease not receiving dialysis. Kidney Int. 2011; 80:112–118. [PubMed: 21451461]
6. Natali A, Vichi S, Landi P, et al. Coronary atherosclerosis in Type II diabetes: angiographic findings and clinical outcome. Diabetologia. 2000; 43:632–641. [PubMed: 10855538]
7. Roijers RB, Debernardi N, Cleutjens JP, et al. Microcalcifications in early intimal lesions of atherosclerotic human coronary arteries. Am J Pathol. 2011; 178:2879–2887. [PubMed: 21531376]
8. New SE, Goettsch C, Aikawa M, et al. Macrophage-derived matrix vesicles: an alternative novel mechanism for microcalcification in atherosclerotic plaques. Circ Res. 2013; 113:72–77. [PubMed: 23616621]
9. Hassan NA, D'Orsi ET, D'Orsi CJ, et al. The risk for medial arterial calcification in CKD. Clin J Am Soc Nephrol. 2012; 7:275–279. [PubMed: 22156752]
10. Lehto S, Niskanen L, Suhonen M, et al. Medial artery calcification. A neglected harbinger of cardiovascular complications in non-insulin-dependent diabetes mellitus. Arterioscler Thromb Vasc Biol. 1996; 16:978–983. [PubMed: 8696962]
11. McEniery CM, McDonnell BJ, So A, et al. Aortic calcification is associated with aortic stiffness and isolated systolic hypertension in healthy individuals. Hypertension. 2009; 53:524–531. [PubMed: 19171791]
12. London GM, Marchais SJ, Guerin AP, et al. Arteriosclerosis, vascular calcifications and cardiovascular disease in uremia. Curr Opin Nephrol Hypertens. 2005; 14:525–531. [PubMed: 16205470]
13. Vlachopoulos C, Aznaouridis K, Stefanadis C. Prediction of cardiovascular events and all-cause mortality with arterial stiffness: a systematic review and meta-analysis. J Am Coll Cardiol. 2010; 55:1318–1327. [PubMed: 20338492]

14. Haase P. The development of nephrocalcinosis in the rat following injections of neutral sodium phosphate. J Anat. 1975; 119:19–37. [PubMed: 1133087]
15. Mackay EM, Oliver J. Renal Damage Following the Ingestion of a Diet Containing an Excess of Inorganic Phosphate. J Exp Med. 1935; 61:319–334. [PubMed: 19870361]
16. Bushinsky DA, Parker WR, Asplin JR. Calcium phosphate supersaturation regulates stone formation in genetic hypercalciuric stone-forming rats. Kidney Int. 2000; 57:550–560. [PubMed: 10652032]
17. Darmon M, Vincent F, Camous L, et al. Tumour lysis syndrome and acute kidney injury in high-risk haematology patients in the rasburicase era. A prospective multicentre study from the Groupe de Recherche en Reanimation Respiratoire et Onco-Hematologique. Br J Haematol. 2013; 162:489–497. [PubMed: 23772757]
18. Chawla LS, Eggers PW, Star RA, et al. Acute kidney injury and chronic kidney disease as interconnected syndromes. N Engl J Med. 2014; 371:58–66. [PubMed: 24988558]
19. Markowitz GS, Nasr SH, Klein P, et al. Renal failure due to acute nephrocalcinosis following oral sodium phosphate bowel cleansing. Human Pathology. 2004; 35:675–684. [PubMed: 15188133]
20. Adeney KL, Siscovick DS, Ix JH, et al. Association of serum phosphate with vascular and valvular calcification in moderate CKD. J Am Soc Nephrol. 2009; 20:381–387. [PubMed: 19073826]
21. El-Abbadi MM, Pai AS, Leaf EM, et al. Phosphate feeding induces arterial medial calcification in uremic mice: role of serum phosphorus, fibroblast growth factor-23, and osteopontin. Kidney Int. 2009; 75:1297–1307. [PubMed: 19322138]
22. Kestenbaum B, Sampson JN, Rudser KD, et al. Serum phosphate levels and mortality risk among people with chronic kidney disease. J Am Soc Nephrol. 2005; 16:520–528. [PubMed: 15615819]
23. Dhingra R, Sullivan LM, Fox CS, et al. Relations of serum phosphorus and calcium levels to the incidence of cardiovascular disease in the community. Arch Intern Med. 2007; 167:879–885. [PubMed: 17502528]
24. Calvo MS, Moshfegh AJ, Tucker KL. Assessing the health impact of phosphorus in the food supply: issues and considerations. Adv Nutr. 2014; 5:104–113. [PubMed: 24425729]
25. Schlieper G, Westenfeld R, Brandenburg V, et al. Inhibitors of calcification in blood and urine. Semin Dial. 2007; 20:113–121. [PubMed: 17374084]
26. Oldberg A, Franzen A, Heinegard D. Cloning and sequence analysis of rat bone sialoprotein (osteopontin) cDNA reveals an Arg-Gly-Asp cell-binding sequence. Proc Natl Acad Sci U S A. 1986; 83:8819–8823. [PubMed: 3024151]
27. Standal T, Borset M, Sundan A. Role of osteopontin in adhesion, migration, cell survival and bone remodeling. Exp Oncol. 2004; 26:179–184. [PubMed: 15494684]
28. Sodek J, Ganss B, McKee MD. Osteopontin. Crit Rev Oral Biol Med. 2000; 11:279–303. [PubMed: 11021631]
29. Chen Y, Bal BS, Gorski JP. Calcium and collagen binding properties of osteopontin, bone sialoprotein, and bone acidic glycoprotein-75 from bone. J Biol Chem. 1992; 267:24871–24878. [PubMed: 1447223]
30. Singh K, Deonarine D, Shanmugam V, et al. Calcium-binding properties of osteopontin derived from non-osteogenic sources. J Biochem. 1993; 114:702–707. [PubMed: 8113224]
31. Mirams M, Robinson BG, Mason RS, et al. Bone as a source of FGF23: regulation by phosphate? Bone. 2004; 35:1192–1199. [PubMed: 15542045]
32. Martin A, Liu S, David V, et al. Bone proteins PHEX and DMP1 regulate fibroblastic growth factor Fgf23 expression in osteocytes through a common pathway involving FGF receptor (FGFR) signaling. FASEB J. 2011; 25:2551–2562. [PubMed: 21507898]
33. Yan X, Yokote H, Jing X, et al. Fibroblast growth factor 23 reduces expression of type IIa Na+/Pi co-transporter by signaling through a receptor functionally distinct from the known FGFRs in opossum kidney cells. Genes Cells. 2005; 10:489–502. [PubMed: 15836777]
34. Isakova T, Wahl P, Vargas GS, et al. Fibroblast growth factor 23 is elevated before parathyroid hormone and phosphate in chronic kidney disease. Kidney Int. 2011; 79:1370–1378. [PubMed: 21389978]
35. Shimada T, Hasegawa H, Yamazaki Y, et al. FGF-23 is a potent regulator of vitamin D metabolism and phosphate homeostasis. J Bone Miner Res. 2004; 19:429–435. [PubMed: 15040831]

36. Shavit L, Girfoglio D, Vijay V, et al. Vascular calcification and bone mineral density in recurrent kidney stone formers. Clin J Am Soc Nephrol. 2015; 10:278–285. [PubMed: 25635036]
37. Mo L, Liaw L, Evan AP, et al. Renal calcinosis and stone formation in mice lacking osteopontin, Tamm-Horsfall protein, or both. Am J Physiol Renal Physiol. 2007; 293:F1935–1943. [PubMed: 17898038]
38. Ohri R, Tung E, Rajachar R, et al. Mitigation of ectopic calcification in osteopontin-deficient mice by exogenous osteopontin. Calcif Tissue Int. 2005; 76:307–315. [PubMed: 15812576]
39. Hirose M, Tozawa K, Okada A, et al. Role of osteopontin in early phase of renal crystal formation: immunohistochemical and microstructural comparisons with osteopontin knock-out mice. Urol Res. 2012; 40:121–129. [PubMed: 21833789]
40. Wesson JA. Osteopontin Is a Critical Inhibitor of Calcium Oxalate Crystal Formation and Retention in Renal Tubules. Journal of the American Society of Nephrology. 2003; 14:139–147. [PubMed: 12506146]
41. Hudkins KL, Giachelli CM, Cui Y, et al. Osteopontin expression in fetal and mature human kidney. J Am Soc Nephrol. 1999; 10:444–457. [PubMed: 10073594]
42. Speer MY, Chien YC, Quan M, et al. Smooth muscle cells deficient in osteopontin have enhanced susceptibility to calcification in vitro. Cardiovasc Res. 2005; 66:324–333. [PubMed: 15820201]
43. Wada T, McKee MD, Steitz S, et al. Calcification of Vascular Smooth Muscle Cell Cultures : Inhibition by Osteopontin. Circulation Research. 1999; 84:166–178. [PubMed: 9933248]
44. Kaartinen MT, Murshed M, Karsenty G, et al. Osteopontin upregulation and polymerization by transglutaminase 2 in calcified arteries of Matrix Gla protein-deficient mice. J Histochem Cytochem. 2007; 55:375–386. [PubMed: 17189522]
45. Matsui Y, Rittling SR, Okamoto H, et al. Osteopontin deficiency attenuates atherosclerosis in female apolipoprotein E-deficient mice. Arterioscler Thromb Vasc Biol. 2003; 23:1029–1034. [PubMed: 12730087]
46. Shao JS, Sierra OL, Cohen R, et al. Vascular calcification and aortic fibrosis: a bifunctional role for osteopontin in diabetic arteriosclerosis. Arterioscler Thromb Vasc Biol. 2011; 31:1821–1833. [PubMed: 21597007]
47. Speer MY, McKee MD, Guldberg RE, et al. Inactivation of the Osteopontin Gene Enhances Vascular Calcification of Matrix Gla Protein-deficient Mice: Evidence for Osteopontin as an Inducible Inhibitor of Vascular Calcification In Vivo. Journal of Experimental Medicine. 2002; 196:1047–1055. [PubMed: 12391016]
48. Fliser D, Kollerits B, Neyer U, et al. Fibroblast growth factor 23 (FGF23) predicts progression of chronic kidney disease: the Mild to Moderate Kidney Disease (MMKD) Study. J Am Soc Nephrol. 2007; 18:2600–2608. [PubMed: 17656479]
49. Schwarz S, Trivedi BK, Kalantar-Zadeh K, et al. Association of disorders in mineral metabolism with progression of chronic kidney disease. Clin J Am Soc Nephrol. 2006; 1:825–831. [PubMed: 17699293]
50. Lochy S, Jacobs R, Honore PM, et al. Phosphate induced crystal acute kidney injury - an under-recognized cause of acute kidney injury potentially leading to chronic kidney disease: case report and review of the literature. Int J Nephrol Renovasc Dis. 2013; 6:61–64. [PubMed: 23662071]
51. Weiss J, Thorp ML. Acute phosphate nephropathy: a cause of chronic kidney disease. BMJ Case Rep. 2011
52. Evenepoel P, Daenen K, Bammens B, et al. Microscopic nephrocalcinosis in chronic kidney disease patients. Nephrol Dial Transplant. 2015; 30:843–848. [PubMed: 25586405]
53. Lorenzen J, Kramer R, Kliem V, et al. Circulating levels of osteopontin are closely related to glomerular filtration rate and cardiovascular risk markers in patients with chronic kidney disease. Eur J Clin Invest. 2010; 40:294–300. [PubMed: 20486990]
54. Barreto DV, Lenglet A, Liabeuf S, et al. Prognostic implication of plasma osteopontin levels in patients with chronic kidney disease. Nephron Clin Pract. 2011; 117:c363–372. [PubMed: 21071960]
55. Yamaguchi H, Igarashi M, Hirata A, et al. Progression of diabetic nephropathy enhances the plasma osteopontin level in type 2 diabetic patients. Endocr J. 2004; 51:499–504. [PubMed: 15516785]

56. Giachelli CM, Bae N, Almeida M, et al. Osteopontin is elevated during neointima formation in rat arteries and is a novel component of human atherosclerotic plaques. J Clin Invest. 1993; 92:1686–1696. [PubMed: 8408622]

57. Matsuzaki H, Katsumata S, Uehara M, et al. High-phosphorus diet induces osteopontin expression of renal tubules in rats. J Clin Biochem Nutr. 2007; 41:179–183. [PubMed: 18299713]

58. Schulte K, Berger K, Boor P, et al. Origin of parietal podocytes in atubular glomeruli mapped by lineage tracing. J Am Soc Nephrol. 2014; 25:129–141. [PubMed: 24071005]

59. Yuan Q, Jiang Y, Zhao X, et al. Increased osteopontin contributes to inhibition of bone mineralization in FGF23-deficient mice. J Bone Miner Res. 2014; 29:693–704. [PubMed: 24038141]

60. Addison WN, Masica DL, Gray JJ, et al. Phosphorylation-dependent inhibition of mineralization by osteopontin ASARM peptides is regulated by PHEX cleavage. J Bone Miner Res. 2010; 25:695–705. [PubMed: 19775205]

61. Massry SG, Coburn JW, Lee DB, et al. Skeletal resistance to parathyroid hormone in renal failure. Studies in 105 human subjects. Ann Intern Med. 1973; 78:357–364. [PubMed: 4571863]

62. Liaw L, Birk DE, Ballas CB, et al. Altered wound healing in mice lacking a functional osteopontin gene (spp1). J Clin Invest. 1998; 101:1468–1478. [PubMed: 9525990]

63. Cockell KA, L'Abbe MR, Belonje B. The concentrations and ratio of dietary calcium and phosphorus influence development of nephrocalcinosis in female rats. J Nutr. 2002; 132:252–256. [PubMed: 11823586]

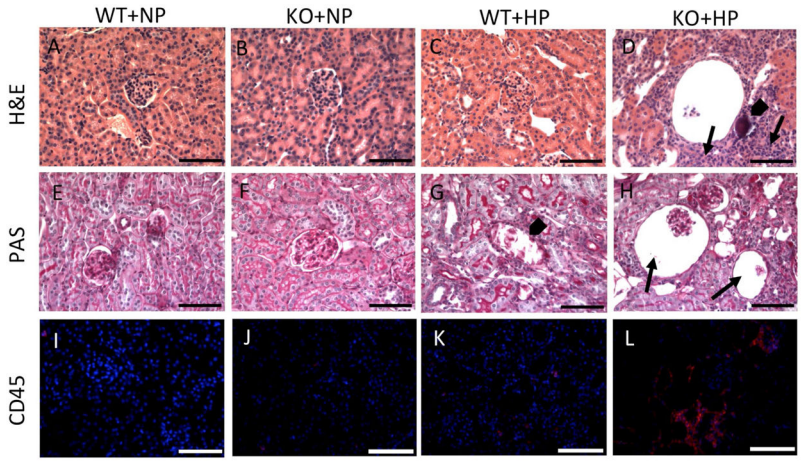

Figure 1. Loss of normal renal structure in the KO+HP group

H&E staining of the WT+NP (A), KO+NP (B), and WT+HP (C) kidneys are normal. H&E staining of the kidneys of the KO+HP group (D) demonstrate a marked cellular infiltrate (arrows) surrounding both dilated tubular structures and mineral deposits (D, arrowhead). PAS staining of the WT+NP (E) and KO+NP (F) kidneys is normal. Occasional tubular mineral deposits are seen on PAS staining of WT+HP kidneys (G, arrowhead) with otherwise normal morphology. PAS staining of KO+HP kidneys (H) demonstrates cystic glomeruli (arrows) with marked dilatation of Bowman's capsule. Dilated tubules are also seen. CD45 IF of the WT+NP (I) and KO+NP (J) indicates the presence of occasional inflammatory cells. The WT+HP group shows mild subcapsular and interstitial inflammation. A significant inflammatory infiltrate is present near cystic, dilated glomeruli and calcification sites (orange in panel L). Original magnification = 20X. Scale bar = 75 μm.

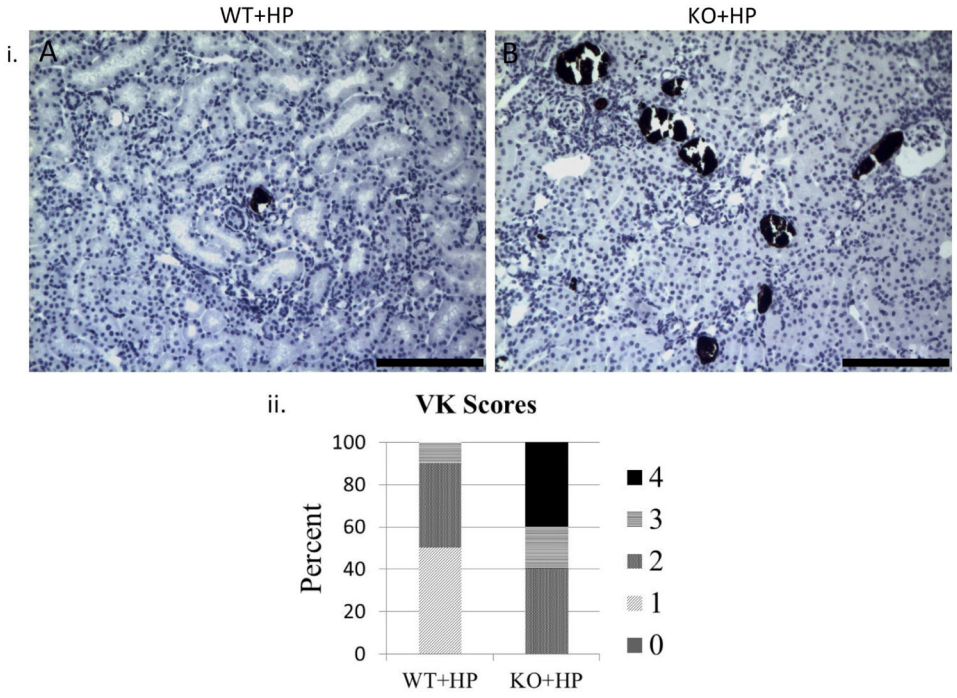

Figure 2. OPN KO mice on HP diet develop abundant renal calcium phosphate deposition

i. VK staining confirms presence of calcium phosphate deposition throughout the kidney of KO+HP mice (B). Occasional renal mineral deposition is seen in the WT+HP mice (A). Original magnification = 10X. Scale bar = 150 μm. ii. VK scoring for mineral granules demonstrates a marked increase in renal calcium deposits in the KO+HP group when compared to the WT+HP group. 0 = no granules found in the section, 1 = 1–25 granules, 2 = 26–75 granules, 3 = 76–150 granules, 4 = >150 granules

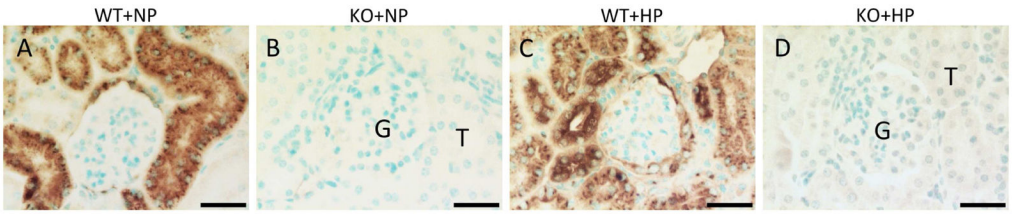

Figure 3. OPN Immunohistochemistry confirms depletion of OPN protein in KO kidney

Kidney sections of WT+NP (A) and WT+HP (C) demonstrate abundant renal tubular OPN expression. OPN expression is absent in the KO+NP (B) and KO+HP (D) kidneys. Original magnification = 40X. Scale bar = 30 μm. G = glomerulus; T = Tubule.

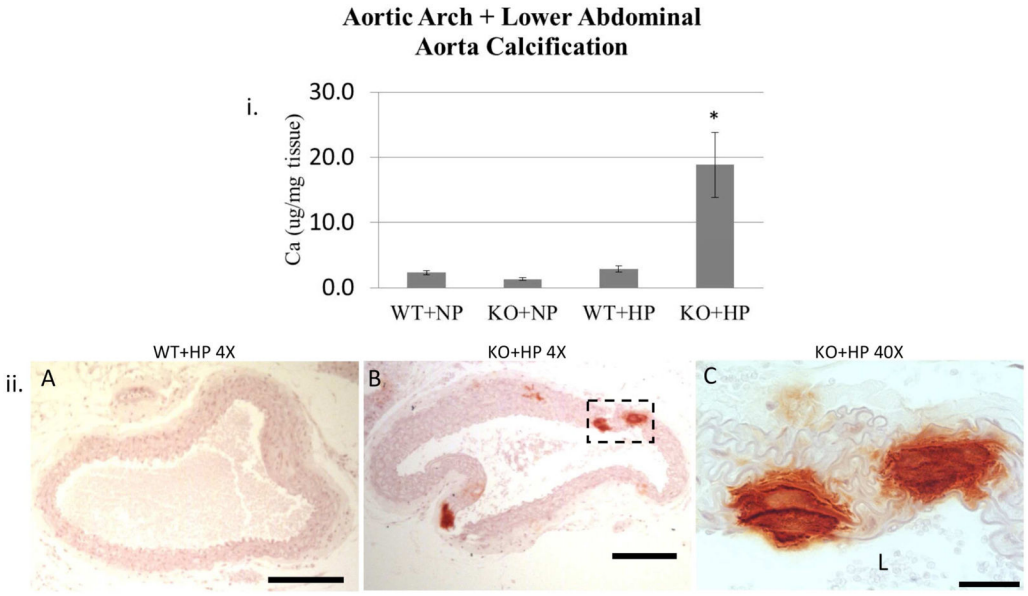

Figure 4. KO+HP mice develop vascular calcification

i. Aortic arch plus lower abdominal aorta biochemical calcium content expressed as μg calcium normalized to mg dry weight (mean±s.e.m.). *$p<0.05$ compared to the WT+NP, KO+NP, and WT+HP. Calcification was not different between the WT+NP, KO+NP, and WT+HP groups. ii. Alizarin Red stains of the abdominal aorta show marked calcification in the KO+HP group (B) and absence of mineral in the WT+HP group (A). Original magnification = 4X (cropped). Scale bar = 350 μm. Magnification of the mineral (box) in the KO+HP aorta (C) shows that the mineral is located entirely in the medial layer of the vessel. Original magnification = 40X. Scale bar = 30 μm. L = lumen.

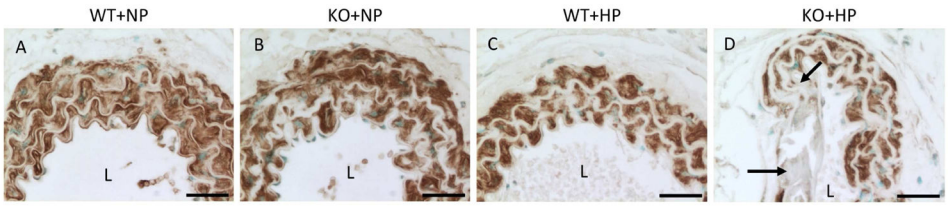

Figure 5. Loss of sm22 alpha expression in the KO+HP aorta confirms phenotypic transformation of VSMCs

Sm22α expression is normal throughout the length of the abdominal aorta in the WT+NP (A), KO+NP (B), and WT+HP (C) groups.) Sm22α expression is absent in areas of the aorta (arrows) in the KO+HP mice (D) consistent with phenotypic transformation of the VSMC seen in vascular calcification. Original magnification = 40X. Scale bar = 30 μm. L = lumen.

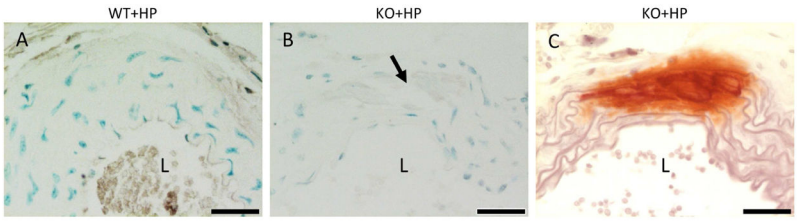

Figure 6. OPN expression is absent in the calcified vasculature of the KO+HP group

OPN IHC of the abdominal aorta of the WT+HP mice (A) demonstrates no OPN expression in the vessel as expected in the absence of calcification. Despite the presence of mineral (arrow) the KO+HP aorta (B) is devoid of OPN. An adjacent section of the KO+HP aorta (C) is stained with Alizarin Red to highlight the mineral. Original magnification = 40X. Scale bar = 30 μm. L = lumen.

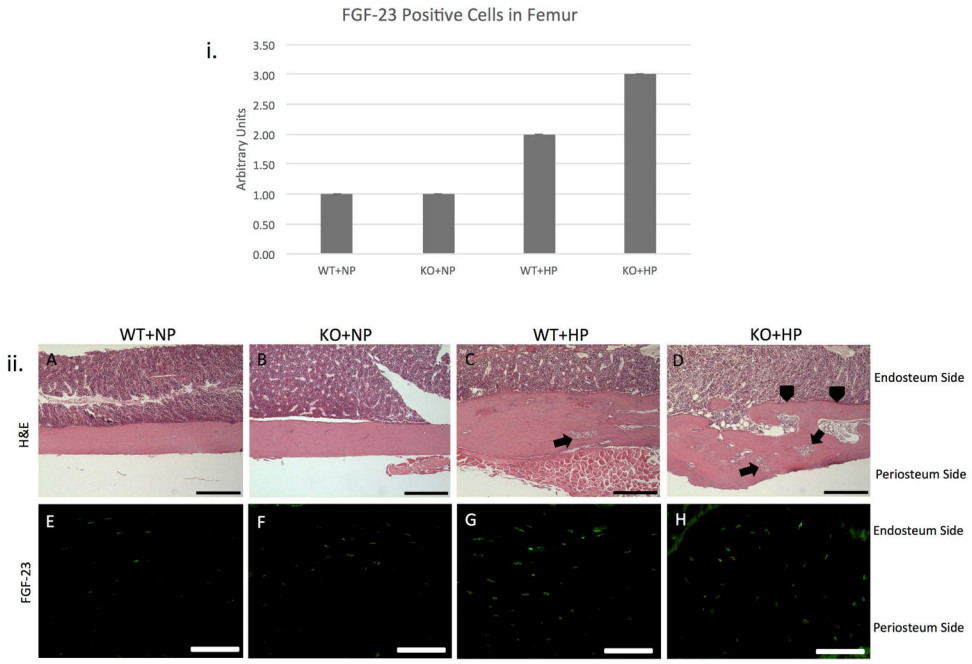

Figure 7. FGF-23 expression is increased in OPN+HP femurs

i. FGF-23 expression is elevated in femurs of WT+HP, but expression is highest in KO+HP. ii. H&E staining of femurs demonstrates widening of the diaphysis and increased cortical porosity (arrows) in both HP fed mice (C,D). Large protrusions of trabeculae (arrowheads) are noted exclusively in the KO+HP group (D). There is more new bone forming in the KO + HP group, and therefore more osteocytes expressing FGF23 per bone area as seen in the IF. H&E: Original magnification = 4X. Scale bar = 350uM. FGF-23 IF: Original magnification = 20X. Scale bar = 75uM.

Table 1

Serum chemistries in the four treatment groups

Treatment Group	n	BUN (mg/dL)	Ca (mg/dL)	P (mg/dL)	PTH (pg/ml)	FGF-23 (pg/ml)
WT+NP	10	26±1	10.7±0.9	9.6±0.3	273±36	423±20
WT+HP	10	30±2[a]	10.6±0.4	7.7±0.6[d]	505±115	1425±215
KO+NP	10	22±1	12.0±0.5	10.8±0.5	399±69	637±76
KO+HP	10	36±2[b]	9.5±0.4[c]	8.3±0.4[e]	714±142[f]	3006±503[g]

Abbreviations: WT, wild-type; KO, osteopontin knockout; NP, normal phosphate diet; HP, high phosphate diet; n, number of mice in each treatment group; BUN, blood urea nitrogen; Ca, calcium; P, phosphorus; PTH, parathyroid hormone; FGF-23, fibroblast growth factor 23.

[a]WT+HP BUN levels were significantly higher when compared to KO+NP ($p<0.05$)

[b]KO+HP BUN levels were significantly higher than WT+NP and KO+NP ($p<0.001$) and WT+HP ($p<0.05$)

[c]KO+HP calcium levels were significantly lower than the KO+NP group ($p<0.05$)

[d]WT+HP phosphate levels were significantly lower than WT+NP ($p<0.05$) and KO+NP ($p<0.001$)

[e]KO+HP phosphate levels were significantly lower than KO+NP ($p<0.05$)

[f]KO+HP PTH levels were increased significantly when compared to the WT+NP group ($p<0.05$)

[g]KO+HP FGF-23 levels were significantly higher than all other groups ($p<0.001$)